Structural and Functional Organization of Human Neocortical Microcircuits

Ph.D. thesis

Réka Barbara Bod, MD

Szentágothai János Neurosciences Division
Semmelweis University

Supervisor: Wittner Lucia, PhD, DSc

Official reviewers: Prof. József Csicsvári, PhD
Péter Ujma, PhD

Head of the Complex Examination Committee:
Prof. Anita Kamondi, MD, DSc

Members of the Final Examination Committee:
Andrea Slézia, PhD
Orsolya Szalárdy, PhD

Budapest, 2026

1. Introduction

The cerebral cortex functions through the interaction of local recurrent circuits and distributed brain-wide networks. Although cortical neurons are organized into highly structured laminar microcircuits, their activity is continuously shaped by corticocortical, subcortical, and neuromodulatory inputs. This means, when coordinated activity is observed in vivo, it is difficult to determine which features arise intrinsically from local circuitry or network embedding.

Acute human cortical slices provide a reduction of this system. Local cellular and synaptic architecture is retained, whereas long-range afferents, neuromodulatory influences, and behavioral context are removed. This makes the preparation useful for separating local circuit mechanisms from network-dependent dynamics. However, isolation is not simply a passive reduction and may itself reorganize cortical activity.

A central assumption of this thesis is that synchronization and integration are related but distinct properties of cortical organization. Local recurrent circuits may engage in population activity and coherent oscillations, whereas broad population integration might depend on interactions with distributed networks. We therefore hypothesized that removal of long-range inputs could reduce network integration without eliminating, and potentially while enhancing, local rhythmic coordination.

2. Objectives

We named our central objective to determine how human cortical microcircuits generate and organize neuronal activity under different levels of network embedding. Adressing this, we pursued two complementary objectives:

Objective I (O1): Epileptic cortical microcircuits.

We aimed to characterize spontaneous population activity and the excitatory components in the local microcircuit organization of the human epileptic neocortex, and to determine how

glutamatergic transmission contributes to the generation and sustenance of spontaneous activity.

Objective II (O2): Network embedding and cortical isolation.

We interrogated features of human cortical dynamics are intrinsic to local circuitry and which depend on long-range network embedding. We compared matched cortical regions during wakefulness, NREM sleep, and after surgical isolation in acute slices, focusing on neuronal firing, spike-field synchronization, population coupling, functional connectivity, network topology, population dimensionality, laminar current-source density, and tissue architecture.

These objectives were designed to distinguish local circuit-generated activity from network-dependent integration while accounting for the structural state of the human cortex.

3. Methods

3.1. Epileptic cortical microcircuits in an excitatory context

O1 examined spontaneous population activity and excitatory microcircuit organization in epileptic and non-epileptic human neocortical tissue. Cortical tissue obtained during therapeutic or clinically indicated resection was transferred immediately to an acute slice preparation. Spontaneous activity was recorded under physiological ACSF, followed by pharmacological manipulation of glutamatergic transmission using the NMDA receptor antagonist APV and combined APV+NBQX blockade of NMDA and AMPA/kainate receptors. Single-unit firing, burst structure, and putative pairwise interactions were quantified alongside laminar histology using NeuN and SMI32 immunostaining.

Spontaneous population activity (SPA) was defined as recurring, synchronous events detected simultaneously in the local field potential and neuronal firing. SPA recurrence, amplitude, and cellular participation were compared between epileptic and non-epileptic tissue and across pharmacological conditions. Firing

rate, inter-spike-interval structure, and burstiness were quantified at the single-cell level, while cross-correlograms were used to identify putative monosynaptic interactions. Histological measurements provided an anatomical reference for neuronal and pyramidal-cell organization.

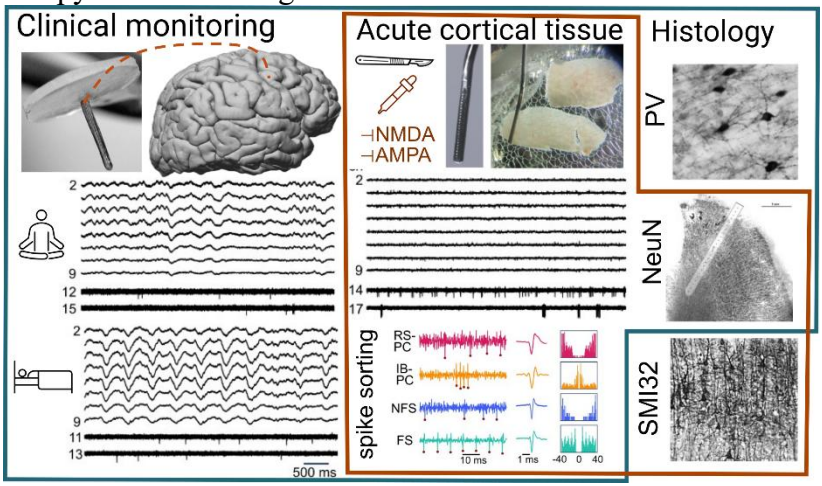


Figure 1. Experimental framework for Objectives I and II.
The two studies share the experimental platform but address distinct questions. Objective I (brick-red frames) examined spontaneous population activity and excitatory microcircuit organization in acute human cortical slices from epileptic and non-epileptic tissue, including pharmacological manipulation of NMDA and AMPA/kainate receptors and NeuN/SMI32 histology. Objective II (teal frames) used a within-patient design in eight patients to compare matched cortical regions during in vivo wakefulness and NREM sleep and following surgical isolation in acute slices. The same laminar microelectrode configuration was used for in vivo and in vitro electrophysiology. Objective II additionally incorporated spike-field synchronization, population coupling, functional connectivity, dimensionality, laminar CSD, and NeuN/PV histology. This distinction is important: O1 and O2 are independent studies with overlapping experimental infrastructure, and not just sequential components of a single experiment.

3.2. Network embedding and cortical isolation

O2 used a within-patient longitudinal design in determining which features of human cortical dynamics depend on

embedding within the intact brain. Eight patients undergoing invasive presurgical monitoring were implanted with a 24-channel linear laminar microelectrode positioned perpendicular to the cortical surface. Single-unit and local field potential activity was recorded during clinically stable wakefulness and NREM sleep. Following therapeutic resection, tissue from the corresponding cortical region was transferred immediately to an acute slice preparation and recorded under otherwise physiological ACSF using the same laminar electrode configuration.

Recordings were analyzed at multiple organizational levels. Single-unit measures included firing rate, action-potential half-width, inter-spike-interval variability, and B20, defined as the proportion of ISIs shorter than 20 ms. Spike–field synchronization was quantified using phase-locking values (PLVs) in low-gamma (30–50 Hz) and high-gamma (50–80 Hz) bands. Population coupling quantified the relationship between individual neuronal activity and the surrounding population, while cross-correlograms were used to estimate putative monosynaptic interactions. Functional relationships were further examined using graph-theoretical measures and population dimensionality.

Laminar current-source density (CSD) and integrated sink strength were used to assess the spatial organization of oscillatory transmembrane currents. Histological analysis of matched tissue examined NeuN-positive neuronal density, PV-positive interneuron density, and PV-positive process coverage before and after acute electrophysiological recording. Finally, a minimal mesoscopic model was used to test whether changes in external drive and local circuit parameters could account for the observed dissociation between gamma synchronization and population integration.

4. Results

4.1 The epileptic human cortex retains spontaneous population dynamics but shows altered excitatory organization

4.1.1. Spontaneous population activity

Isolated human cortical tissue generated recurring spontaneous population activity in both epileptic and non-epileptic samples. Population events occurred at approximately 1 Hz, with comparable LFP and multiunit amplitudes between groups, indicating that spontaneous population activity was not itself a specific signature of epileptic tissue.

4.1.2. Pharmacology reveals altered excitatory dependence

Blocking NMDA receptors with APV reduced spontaneous population activity in epileptic tissue and showed a similar trend in non-epileptic tissue, whereas combined glutamatergic receptor blockade abolished activity in both groups. These findings indicate that glutamatergic transmission is essential for recurrent population activity and support a role for NMDA receptor-dependent mechanisms in its maintenance.

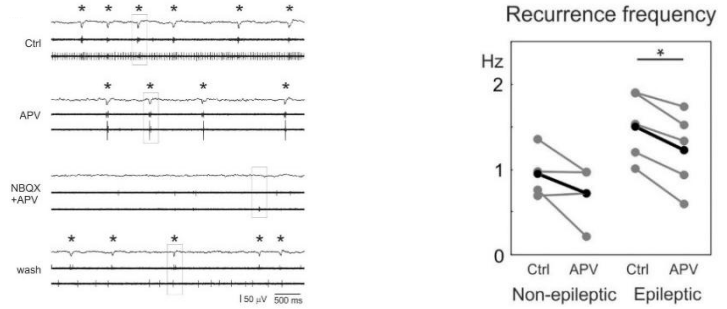


Figure 2. Glutamatergic mechanisms underlying spontaneous population activity in Objective I. Representative spontaneous population activity (SPA) and simultaneous single-unit activity recorded from non-epileptic human neocortex during control ACSF, NMDA receptor blockade with APV, combined NMDA and AMPA/kainate receptor blockade with APV+NBQX, and washout. SPA recurrence frequency was significantly reduced by APV in epileptic tissue, whereas combined blockade abolished SPA in both tissue groups and activity recovered following washout.

4.1.3. Cellular and circuit organization

Epilepsy did not produce a generalized increase in firing rate. Instead, differences were concentrated in specific cellular and circuit features: granular-layer neurons showed higher firing rates, and epileptic neurons displayed greater burstiness.

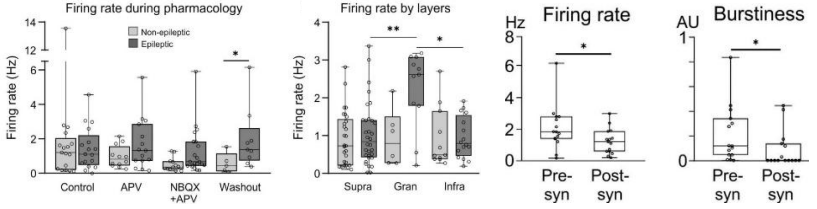


Figure 3. Altered neuronal firing and burst organization in epileptic human neocortex.Single-unit firing rates across supragranular, granular, and infragranular layers in epileptic and non-epileptic tissue. Additional analyses characterize burstiness and firing properties of neurons participating in putative functional interactions, revealing selective alterations in firing and burst structure instead generalized hyperexcitability.

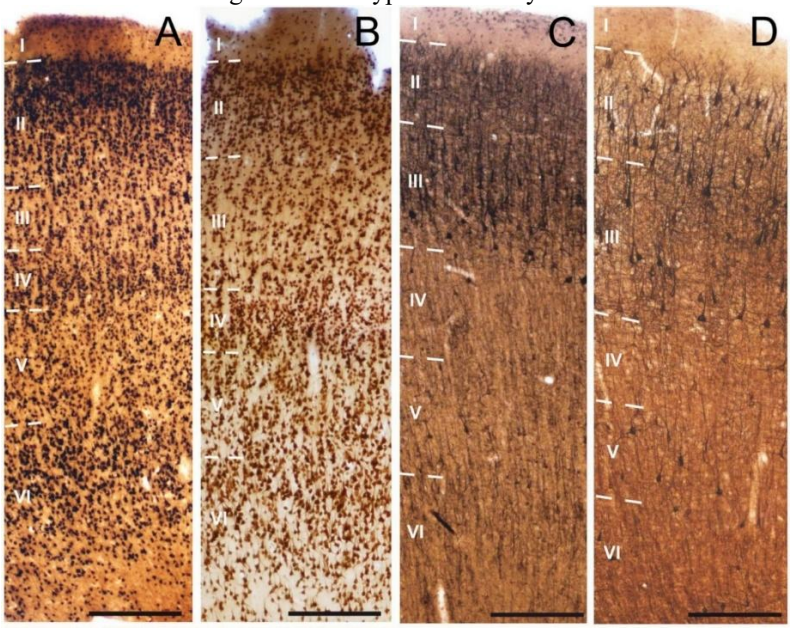


Figure 4. Preserved neuronal and pyramidal-cell architecture in epileptic human neocortex. Representative NeuN and SMI32 immunostaining from

non-epileptic and epileptic cortical tissue. NeuN staining demonstrates preserved laminar organization, while SMI32 identifies projecting pyramidal neurons. Quantification shows no significant difference in SMI32-positive pyramidal-cell density between tissue groups.

Putative monosynaptic interactions were sparse overall, but intrinsically bursting principal cells were disproportionately represented among detected interactions, particularly as presynaptic elements. Histological analysis showed preserved laminar organization and no significant difference in SMI32-positive pyramidal-cell density between groups.

Together, these findings suggest that epileptic cortex retains the structural substrate required for organized spontaneous activity but operates with altered excitatory recruitment and temporal organization instead of a simple global increase in neuronal excitability.

4.2 Cortical isolation increases local synchronization while reducing network integration

4.2.1. Cortical isolation changes neuronal operating properties without suppressing spontaneous activity

We next asked which features of human cortical activity depend on continued embedding within the intact brain. The same cortical regions were examined across three experimental conditions: wakefulness, NREM sleep, and acute cortical isolation. Isolation altered several intrinsic electrophysiological properties. Extracellular action potentials became broader, with median half-width increasing from a median of ~ 0.21 ms in vivo to 0.37 ms in vitro. Maximum firing rates also increased, particularly among principal cells. In contrast, baseline spontaneous firing rates showed comparatively modest changes, and longitudinally tracked neurons did not exhibit a uniform state-dependent trajectory between wakefulness and NREM sleep. Thus, cortical isolation did not simply suppress neuronal activity. Instead, it altered the operating regime of individual neurons while preserving substantial spontaneous firing.

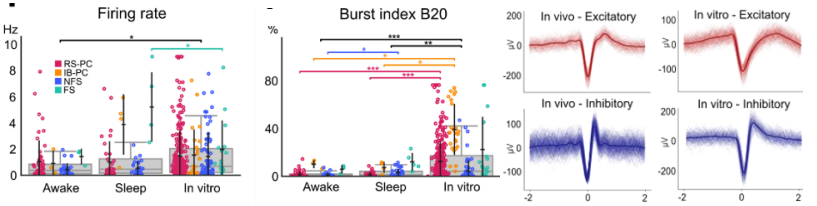


Figure 5. Single-unit electrophysiological properties across network states in Objective II. Representative extracellular action-potential waveforms and quantitative measures of firing rate, maximum firing rate, action-potential half-width, and B20 across wakefulness, NREM sleep, and acute in vitro isolation. B20 denotes the proportion of inter-spike intervals shorter than 20 ms. Cortical isolation was associated with action-potential broadening and increased maximal firing output while preserving substantial spontaneous activity.

4.2.2. Gamma synchronization increases progressively from wakefulness to isolation

The strongest change emerged at the level of spike-field coordination. Gamma-band phase locking increased progressively across the experimental axis. Low-gamma PLV increased from approximately 0.075 during wakefulness to 0.120 during NREM sleep and 0.369 in vitro. High-gamma phase locking showed a similar trajectory. This increase was observed across most functional cell classes, with NFS interneurons showing a distinct pattern. The wake-to-sleep transition already produced an increase in gamma coupling in longitudinally tracked units, indicating that the isolated preparation did not create an entirely novel form of synchronization. More importantly, isolation strongly amplified a tendency toward local rhythmic coordination that was already expressed during NREM sleep. Importantly, laminar CSD showed that gamma-related sink-source organization remained spatially organized across all three conditions. High-gamma laminar organization was particularly preserved. Increased phase locking therefore occurred despite a reduction in low-gamma integrated sink strength, arguing against a simple

interpretation in which stronger spike–field coupling reflects proportionally stronger bulk transmembrane current.

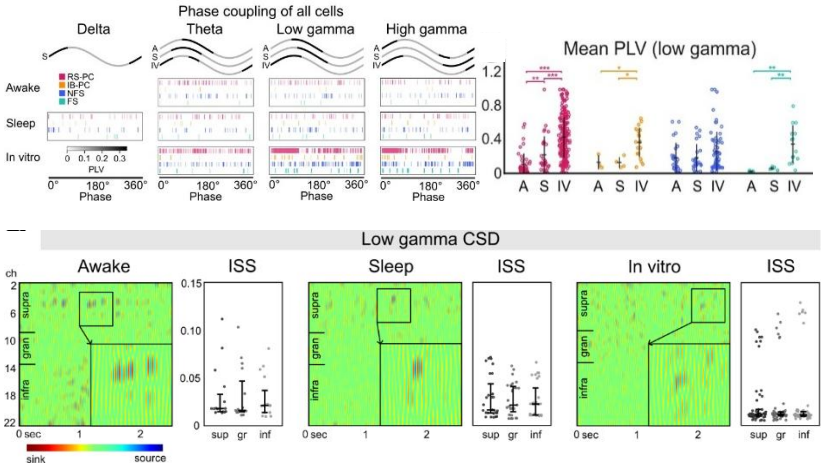


Figure 6. Gamma spike–field synchronization and laminar current organization across network states. Preferred spike phases of significantly phase-locked units across delta, theta, low-gamma, and high-gamma frequency bands in wakefulness (A), NREM sleep (S), and acute isolation (IV). Each raster represents one unit; cell class and coupling strength are indicated by the corresponding color scale. Black lines indicate the population mean preferred phase. Representative laminar low-gamma LFP and CSD profiles and integrated sink strength (ISS) are shown across conditions. Gamma phase locking increased from wakefulness to sleep and was further enhanced in vitro, despite preserved laminar sink–source organization and reduced low-gamma ISS.

4.2.3. Increased synchronization is accompanied by reduced population integration

Population coupling decreased substantially following cortical isolation. Putative monosynaptic interactions were also markedly reduced, from approximately 1.38% of tested pairs in vivo to 0.18% in vitro. Functional network structure became increasingly modular rather than globally integrated. Population dimensionality showed the same direction of change. Participation ratio and eigenspectrum entropy decreased, whereas the proportion of population variance explained by the

first principal component increased. These complementary measures indicate that neuronal activity occupied a progressively more constrained state space following isolation. Together, these findings reveal a dissociation between two properties that are often treated as closely related: gamma synchronization increased, while population integration and dynamical dimensionality decreased. The isolated cortex therefore became more rhythmically coordinated but less globally integrated.

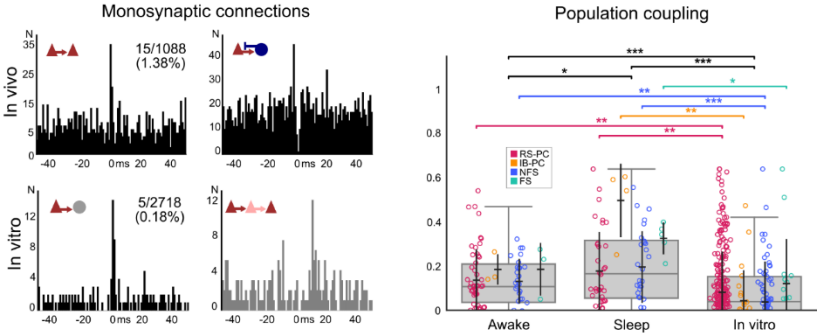


Figure 7. Reduced functional interaction structure following cortical isolation. Representative cross-correlograms illustrating putative excitatory monosynaptic, excitatory–inhibitory, and delayed polysynaptic interactions. Population coupling is shown across wakefulness, NREM sleep, and acute isolation for each functional cell class. Cortical isolation was associated with a marked reduction in population coupling and putative monosynaptic interactions.

4.2.4. Preserved cellular architecture does not imply preserved network function

Histological analysis provided an important control for tissue deterioration as an explanation for the physiological changes. NeuN-positive neuronal density retained the expected laminar organization, with higher density in supragranular cortex, and was largely preserved between tissue examined immediately after resection and tissue examined following acute electrophysiological recording. PV-positive cell density was

likewise preserved. PV process coverage, however, showed a modest reduction following isolation, indicating compromise of PV-positive dendritic and axonal elements despite preservation of the underlying neuronal population. This finding is particularly relevant to the gamma result. PV interneurons are strongly associated with cortical oscillatory coordination, but the reduction in PV process coverage was accompanied not by weaker gamma phase locking but by a marked increase. Thus, the data do not support a simple one-to-one relationship between PV structural integrity and measured gamma synchronization.
The loss of PV processes may nevertheless contribute to the reduction in population coupling by altering local inhibitory connectivity. Together with the removal of long-range afferents, such structural changes could reshape the balance between local synchronization and broader population integration.

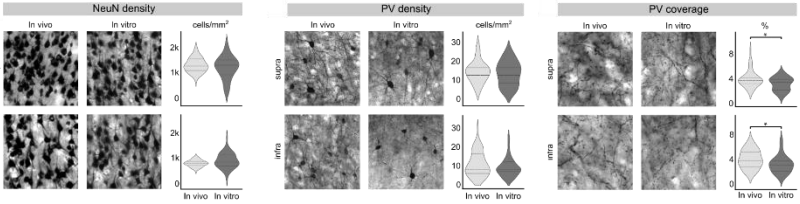


Figure 8. Preservation of neuronal and PV-positive cell density with reduced PV process coverage after isolation. Representative supragranular and infragranular micrographs from tissue fixed immediately after resection and following acute in vitro electrophysiology. NeuN-positive neuronal density and PV-positive cell density were largely preserved, whereas PV process coverage showed a modest reduction following isolation.

4.2.5. The relationship between anatomy and function changes after isolation

We next examined whether preserved local anatomy continued to predict physiological organization. In vivo, NeuN density was positively associated with population coupling, indicating that regions with greater neuronal density were more strongly embedded in ongoing population activity. After isolation, this relationship weakened and reversed. Because of the limited

number of histological samples, the individual correlations should not be interpreted as definitive population-level effects. Reasonably, the important observation is the change in the structure–function relationship across experimental conditions. The same cortical architecture therefore does not have a fixed functional meaning independent of network context. Long-range embedding determines how local structural resources participate in population-level dynamics.

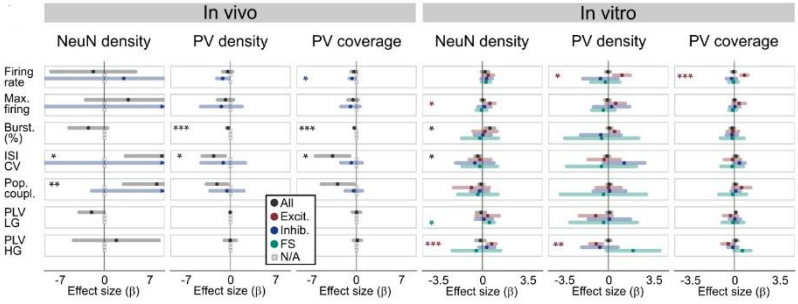


Figure 9. Network embedding alters structure–function relationships. Standardized coefficients from mixed-effects models relating NeuN density, PV density, and PV process coverage to single-unit and population-level physiological measures. NeuN density was positively associated with population coupling in vivo, whereas this relationship weakened or reversed following isolation. Error estimates represent 95% confidence intervals; significance values are FDR corrected.

4.2.6. A minimal model reproduces the synchrony–integration dissociation

Finally, we asked whether the observed dissociation could arise from a small number of interpretable circuit-level changes. A minimal mesoscopic model incorporated spatially constrained recurrent connectivity, excitatory and inhibitory interactions, external drive, PV-related axonal survival, local resonance, and observation noise. Model parameters were optimized separately for wakefulness, NREM sleep, and in vitro conditions against the empirical population-coupling and gamma-PLV measures.

The model reproduced the central experimental transition: population coupling decreased while gamma phase locking increased following deafferentation. Sensitivity analysis further indicated that population coupling was dominated by parameters controlling external drive, whereas gamma phase locking was more strongly influenced by local resonance and PV-related parameters. In conclusion, the model provides a mechanistic proof-of-principle for the experimental observation: removal of long-range network input can reduce population integration without eliminating local rhythmic coordination. Indeed, under altered local circuit conditions, rhythmic synchronization can become stronger as integration declines.

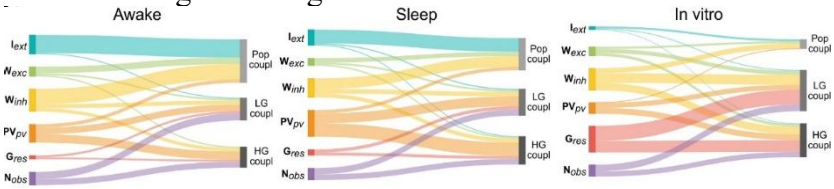


Figure 10. Minimal model of the synchronization–integration dissociation. Model decomposition showing the contributions of six latent parameters: external drive (g_{ext}), recurrent excitation (g_E), recurrent inhibition (g_I), PV axonal survival (s_{PV}), resonance gain (g_{res}) and observation noise (σ_{obs}) to population coupling and gamma phase locking. The model reproduces the empirical decrease in population integration alongside increased gamma synchronization following cortical deafferentation.

5. Conclusions

This thesis shows that human cortical microcircuits retain substantial capacity for organized neuronal activity after removal from the intact brain, but that isolation fundamentally changes how this activity is organized.

Objective I demonstrated that epileptic and non-epileptic human cortex can generate spontaneous population activity through recurrent glutamatergic mechanisms. Epileptic tissue showed altered bursting and increased dependence on NMDA receptor-mediated transmission, indicating functional reorganization

without evidence for widespread loss of the excitatory neuronal scaffold.

Objective II demonstrated a distinct principle: cortical isolation increased gamma spike–field synchronization while reducing population coupling, putative connectivity, and dynamical dimensionality. This dissociation occurred despite preserved neuronal and PV cell densities, although PV-positive process coverage was reduced.

Taken together, the findings distinguish local synchronization from network integration. Local cortical circuits can generate and amplify coherent rhythms, whereas large-scale network embedding contributes to the integration and dynamical diversity of cortical activity. The intact brain therefore does not merely drive cortical neurons; it determines how locally generated activity is incorporated into a broader population state.

6. Bibliography of the candidate's publications

Publications related to the thesis:

1. Bod RB, Rokai J, Meszéna D, Fiáth R, Ulbert I, Márton G. From End to End: Gaining, Sorting, and Employing High-Density Neural Single Unit Recordings. Frontiers in Neuroinformatics. Frontiers Media S.A.; 2022.

2. Bod R, Tóth K, Essam N, Tóth EZ, Erőss L, Entz L, et al. Synaptic alterations and neuronal firing in human epileptic neocortical excitatory networks. Front Synaptic Neurosci. Frontiers Media SA; 2023; 15.

3. (preprint):
Bod R, Tóth K, Farkas O, Michaeli Y, Tóth KZ, et al. Cortical isolation separates rhythmic synchrony from network integration in the human neocortex.

Publications not related to the thesis:

1. Mihály I, Berki ÁJ, Orbán-Kis K, Gáll Z, Bod RB, Szilágyi T. The effect of amygdala low-frequency stimulation on inter-

hippocampal connectivity in the pilocarpine model of epilepsy. Acta Marisiensis - Seria Medica. Sciendo; 2021; 67(1):27–33.
2. Mihály I, Orbán-Kis K, Gáll Z, Berki ÁJ, Bod RB, Szilágyi T. Amygdala low-frequency stimulation reduces pathological phase-amplitude coupling in the pilocarpine model of epilepsy. Brain Sci. MDPI AG; 2020; 10(11):1–18.
3. Mihály I, Molnár T, Berki Á-J, Bod RB, Orbán-Kis K, Gáll Z, et al. Short-Term Amygdala Low-Frequency Stimulation Does not Influence Hippocampal Interneuron Changes Observed in the Pilocarpine Model of Epilepsy and Technology of Târgu Mures [Internet]. 2021. Available from: https://doi.org/10.3390/cells10030520.
4. Gáll Z, Kelemen K, Tolokán A, Zolcseak I, Sável I, Bod R, et al. Anticonvulsant Action and Long-Term Effects of Chronic Cannabidiol Treatment in the Rat Pentylenetetrazole-Kindling Model of Epilepsy. Biomedicines. MDPI; 2022; 10(8).
5. Mihály I, Bod R-B, Orbán-Kis K, Berki Á-J, Szilágyi T. The Effect of Deep Brain Stimulation on High Frequency Oscillations in a Chronic Epilepsy Model. Bulletin of Medical Sciences. Walter de Gruyter GmbH; 2020; 93(2):63–70.
6. Tóth EZ, Stelcz R, Bod R, Petik Á, Juhász E, Tóth K, et al. Adaptive Network Stabilization Despite Profound Structural Reorganization in Human Organotypic Cultures, Advanced Science, 2026.

∑IF: 36,16